MICROWAVE LIMITERS

A microwave limiter is designed to allow low-power signals to pass through it, while attenuating high-power signals. Stated another way, microwave limiters are power-dependent attenuators that prevent intense microwave energy from interfering with susceptible microwave components in the latter stages of a cascade.

Most limiters operate by reducing the impedance of a transmission line when the incident power is above the threshold power level, reflecting or absorbing the incident power. Although, in most cases, a limiter reflects the majority of the intense incident power back toward the power source on the transmission line, where a circulator, an isolator, or a hybrid coupler may divert or absorb it, a microwave limiter may also be designed to absorb the incident power in the same manner as a microwave switch.

In most applications, microwave limiters (sometimes referred to as receiver protectors and terminal-protection devices) are located near the antenna port. However, limiters have also been used in intermediate frequency channels, where signals from a number of channels are combined to create an intense signal (e.g., the intermediate frequency circuit of a phased-array radar). In radar applications, the term "duplexer" is sometimes used to refer to the front-end receiver protection circuitry.

Many microwave limiter technologies have been investigated over the previous half-century. The common technologies are identified in Table 1. The solid-state limiter, which was first designed using the varactor diode, today employs the Si *p–i–n* (or PIN) diode [see (1) and DIODES], because of the *p–i–n*'s lower capacitance per unit area resulting in better thermal characteristics, in addition to the fact that it requires no external power supply. Also shown in the table is the fact that a MESFET-based, MMIC-compatible microwave limiter is being developed for integration with the low-noise amplifiers common in MMIC designs. Furthermore, although gaseous limiters are widely used in high-power radars as receiver protectors, ferrite limiters have not found the same wide use.

SOLID-STATE LIMITERS

At radio frequencies, it is common to place back-to-back signal diodes (e.g., 1N914) shunted to ground across the input transmission line of a radio receiver, as shown in Fig. 1(a). When the peak voltage on the line exceeds the forward conduction voltage (typically, 0.7 V) the transmission line voltage is clipped. Below the threshold voltage, the diodes appear as shunt capacitors across the line [see DIODES]. The high capacitance of the 1N914 prevents the extension of this design to microwave frequencies, where the capacitive reactance becomes very low, yielding an undesirable impedance discontinuity, shunting the transmission line that must be tuned out to retain a small voltage standing wave ratio (*VSWR*) at low line voltages. The additional reactance narrows the bandwidth of the transmission line, which may be unacceptable.

Table 1. Common Microwave Limiter Technologies

Technology	Common Implementations
Solid-state	*p–i–n* diode
	MESFET
Gaseous	Waveguide
	Stripline
Ferrite	Filter
	Stripline

p–i–n Diode Limiter

The *p–i–n* diode has a lower capacitance for a given cross-sectional area than other diode designs, because the distance between the *p*+ and *n*+ regions is separated with the *i*-region, whereas in other signal diodes, only the depletion region separates the two highly doped regions. The *i*-region thickness of a *p–i–n* diode is, typically, in the 1 μm to 200 μm range, whereas other diode depletion regions are, typically, less than 2 μm. A good measure of the *i*-region thickness (h) is the reverse breakdown voltage (V_b) at a few microamperes. Several relations are used, including $V_b = 36h^{0.81}$ [Ward et al. (2)] and the simpler rule-of-thumb $V_b = 20h$ for $h \geq 5$, where V_b is in volts and h is in micrometers.

Since the capacitance of a parallel plate capacitor is inversely proportional to the separation distance of the charged plates (represented by the *p*+ and *n*+ charge regions), the *p–i–n* diode has significantly lower capacitance per unit area at zero bias than a signal diode. This feature allows the *p–i–n* diode to be a high-reactance connected in shunt across a transmission line even at microwave frequencies, yielding low insertion loss. The feature also provides more volume than a signal diode for dissipating heat from intense incident pulses.

The *i*-region changes the terminal current–voltage relationship [see DIODES], as compared to other minority-carrier (e.g., signal) or majority-carrier (Schottky) diodes. Varactor diodes have carrier distributions similar to thin *i*-region *p–i–n* diodes. For this reason, varactor diodes were used as limiter diodes until the special doping profile of the *p–i–n* was developed. Leenov (3) studied the *p–i–n* diode configuration and determined that, at frequencies lower than the inverse transit time of the *i*-region, the diode rectifies with a low series resistance. At very high frequencies, the charge distributions at the edges of the *i*-region oscillate with the applied terminal voltage; however, since carriers do not have time to transit the *i*-region, the current is primarily a displacement current and the diode impedance remains high. Leenov found that, when excited with a sine wave, the diode resistance is

$$R_j = \frac{10^{-4}kTh}{q(D/2\pi\ f)^{1/2}}\sqrt{\frac{Z_o}{P_i}}\ \Omega \qquad (1)$$

where k is Boltzmann's constant (1.38×10^{-23} W · s/K), T is the absolute temperature (K), q is the electron charge (1.6×10^{-19} C), D is the diffusion coefficient (15.6 cm^2/s for Si), Z_0 is the impedance of the transmission line in ohms, h is the I-region thickness in microns, and P_i is the incident power in watts. Garver (4) uses Eq. (1) to show that the attenuation α provided by a single diode across a

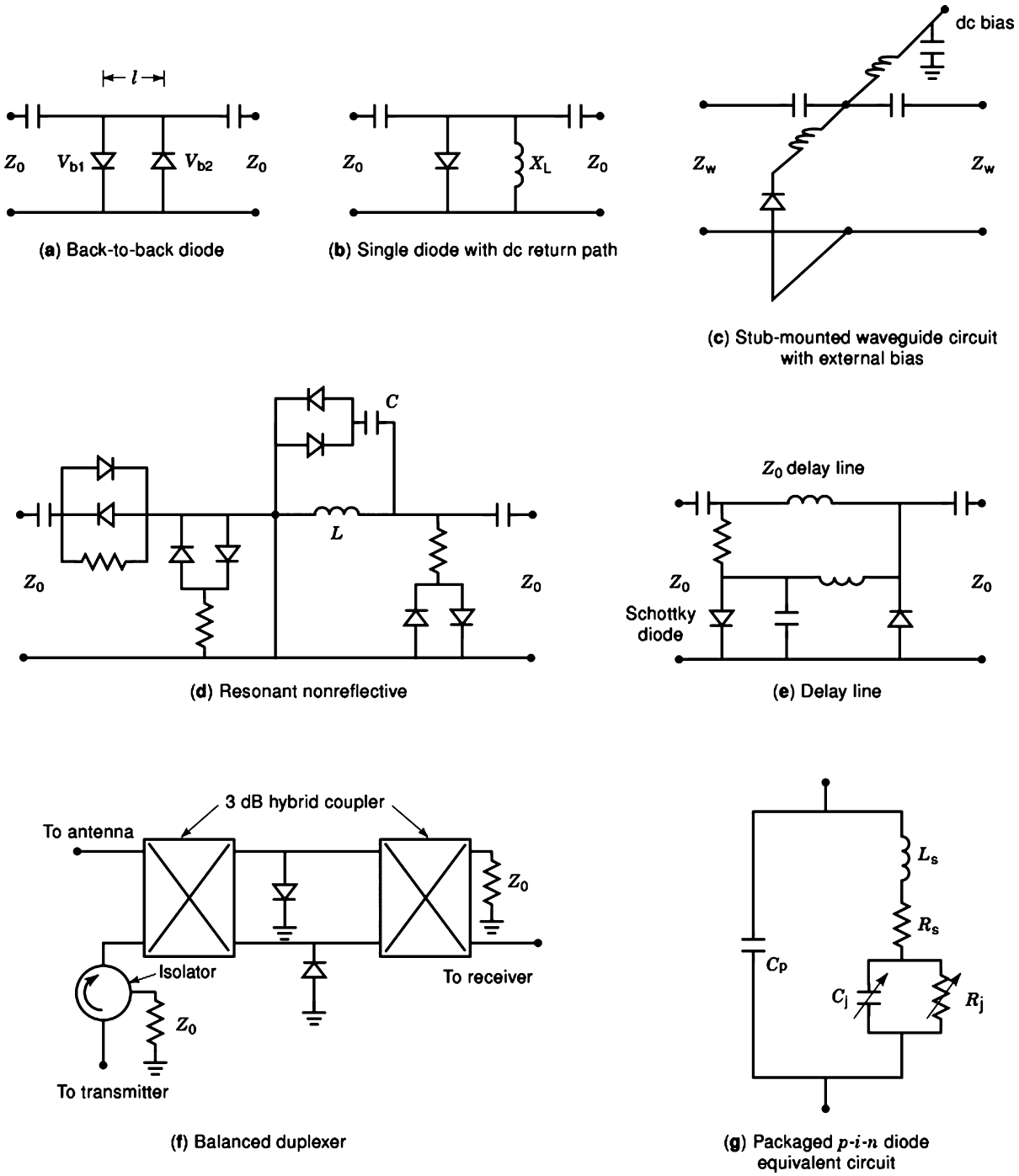

Figure 1. Diode limiter equivalent circuits.

transmission line is

$$\alpha = 10 \times \log_{10}\left[1 + \frac{(q/kT)^2\, DZ_o P_i}{(8 \times 10^{-8})\pi\ fh^2}\right] \text{ dB} \qquad (2)$$

The attenuation is proportional to the $\log(1/fh^2)$ for a given impedance and p–i–n device material. For example, consider a Si PIN diode in a 50-ohm limiter circuit similar to Figure 1b with a 10-GHz incident pulse of 1 W at 290 K (hence $q/kT = 40$). The i-region thickness of the diode is 20 μm. Using Eq. 1, R_j = 22 ohms and the attenuation from Eq. 2 yields 3.5 dB. This low level of attenuation arises because of the 20 μm i-region thickness. Reducing h to 2 μm yields R_j = 2.2 ohms and α = 21 dB. These calculations do not include the effects of the junction capacitance C_j and the package parasitics shown in Fig 1g.

At higher frequencies, the h must be reduced to provide the same level of attenuation, resulting in a higher shunt capacitance per unit area for the diode and increased low-power level attenuation or bandwidth limiting. To compensate for this effect, the cross-sectional area

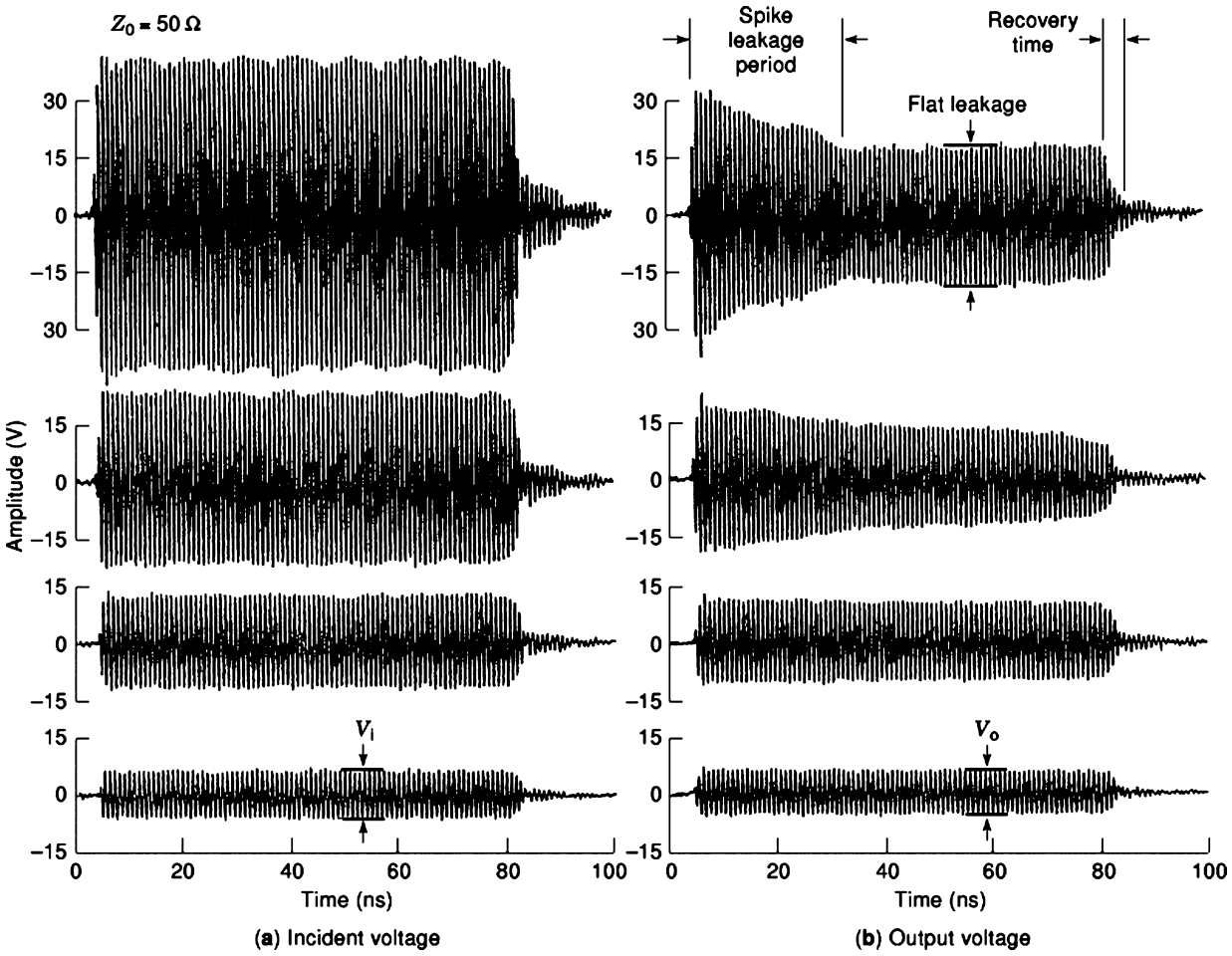

Figure 2. Incident and output voltage–time waveforms for a *p–i–n* diode limiter.

of the diode is reduced. Brown (5) showed that the device thicknesses should be less than about 25 μm at 0.1 GHz to 2.5 μm at 10 GHz in order to avoid high spike leakage, high power absorption during the transition from the high-impedance diode state to the low-impedance diode state, and low insertion loss at low signal levels. Spike leakage is the momentary power that passes through the limiter before the diode's impedance reduces, thus reflecting the incident power back toward the source. Fast-risetime, incident pulses will appear to have a "spike" of leakage power at the output of the limiter.

Since the performance of the *p–i–n* diode depends on the ability of carriers to transit the *i*-region, transient effects occur that are dependent on frequency and other parameters (e.g., *i*-region doping density). For example, Fig. 2 shows the voltage–time waveform of a limiter consisting of two 20 μm Si *p–i–n* diodes closely spaced in shunt with a 50-ohm transmission line as shown in Fig. 1(a) with $l \cong 0$ at four incident voltage amplitudes. Note that this circuit is shown only to present the concept; actual limiters might use thinner *i*-region diodes arranged in another configuration [see Fig. 1(b–f)]. All these circuits allow rectified current to flow through both diodes. Leenov (3) showed that a dc current is much more efficient in lowering the *p–i–n* diode's impedance than an RF current. Unless this rectified current is allowed to flow in a low-impedance circuit (typically less than 5 Ω), the *p–i–n* diode resistance may not be reduced to a few ohms (typical). The voltage–time waveforms on the left in Fig. 2 are the incident voltage at 1.1 GHz, and the waveforms on the right are the voltage following the dual-diode limiter. The *p–i–n* diodes do not clip the incident wave as would a high-speed signal diode; rather, their impedance is reduced by injection of carriers into the *i*-region. At the lowest incident voltage V_i, the attenuation (insertion loss) of the limiter is $20\log_{10}(V_o/V_i) \approx -1$ dB, where V_o is the output voltage. As the V_i is doubled, the V_o tends to show an initial transmission transient (termed spike leakage), followed by a relatively constant output voltage (termed flat leakage). It requires tens of nanoseconds for the two diodes to lower their impedance below the Z_o of the transmission line. However, the spike leakage period would be much more rapid if the *i*-region was thinner or the 20 μm diodes were excited at a lower frequency. The amount of energy in this period (i.e., the integral of the power–time profile) is the spike energy that may destroy susceptible microwave devices in cascade with the limiter. As a rule-of-thumb, low-noise, microwave amplifiers will be destroyed if the spike energy exceeds 1 μJ, and destruction of microwave mixers will occur at the 10 μJ level. If the spike energy must be reduced, the

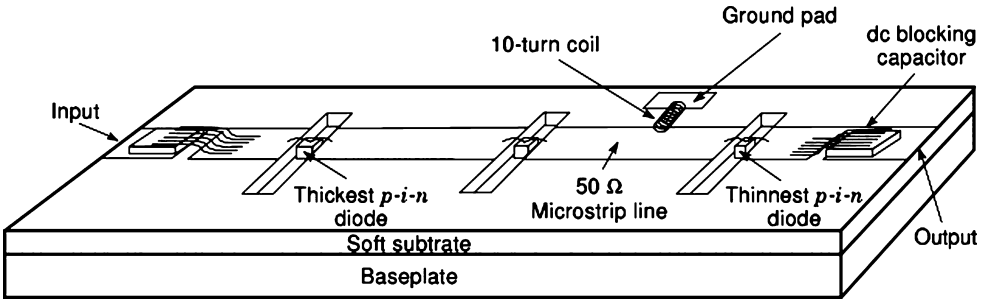

Figure 3. Sketch of a multistage *p–i–n* diode limiter.

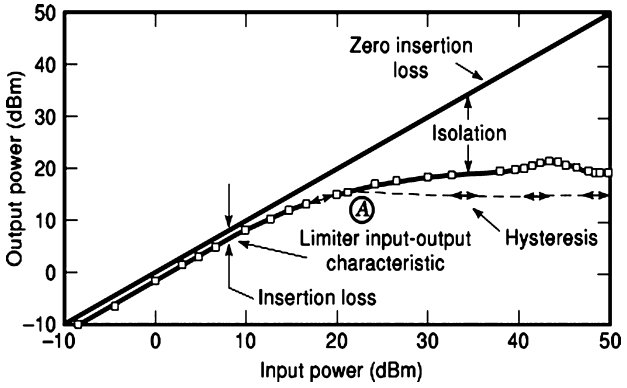

Figure 4. Input–output power characteristic of a *p–i–n* diode limiter.

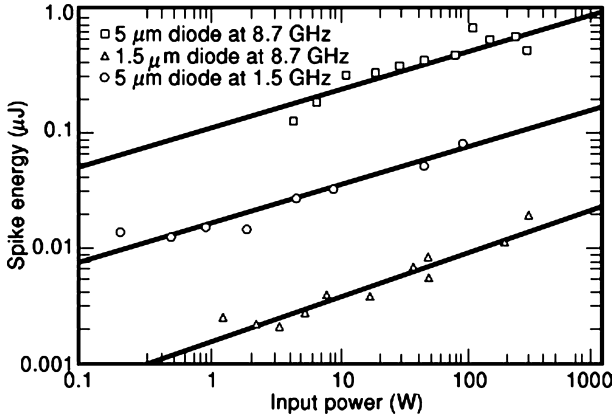

Figure 5. Spike energy for 1.5 μm and 5 μm thick *i*-region *p–i–n* diodes.

second limiter diode with a thinner *i*-region is located a quarter wavelength behind the first limiter diode as shown in Fig. 1(a) with l = ¼ wavelength.

A commercial limiter using three *p–i–n* diodes shunting a soft-substrate, 50-ohm transmission line is shown in Fig. 3. The thinnest *p–i–n* diode is located near the output receiver port, of the limiter and activates first, setting the threshold for limiting. The 10-turn coil allows the rectified current to flow through the diode(s). The standing wave reflected from the thinnest diode excites the middle diode, and the thickest diode is activated at higher incident power levels. At signal levels below threshold, the bandwidth (defined by VSWR $\leq$ 1.6:1) of this limiter design is 2 GHz to 8 GHz, with an insertion loss less than 1.3 dB. The limiter is specified to sustain a 3 W continuous incident power, with 0.1 W output level. The input–output curve measured at 2 GHz for the commercial limiter (shown in Fig. 4) confirms the flat leakage level at 0.1 W, and the insertion loss at less than 1 dB at the low end of the operating band. The input 1 dB compression point was measured to be 11 dBm, and the input third-order intercept was 18 dBm at 3 GHz and was 15 dBm at 7 GHz. During pulsed operation, the unit will sustain a 1000 W pulse train, with a 1 μs length and a 1% duty cycle. The recovery time (defined as the time to return to low insertion loss after the high incident power is removed) is specified as less than 1 μs.

Spike Leakage

The data in Fig. 2 show that the peak spike leakage power increased and the duration of the spike decreased with increasing incident voltage. The measured spike energy for 1.5 and 5 μm *i*-region diodes is shown in Fig. 5. Calculations supporting these results (2) show that a slightly *p*-doped (10^{15} cm^{-3}) intrinsic region would exhibit less spike leakage than the usual *n*-doped (10^{14} cm^{-3} or less) intrinsic region. This result arises because a higher density of the lower mobility holes yields a lower impedance *i*-region than the usual case with the *n*-doped *i*-region.

Caverly and Quinn (6) have develop a SPICE model incorporating the i-region charge storage effects. Their model shows the spike and flat leakage behaviors in addition to the recovery effects.

Recovery Time

The recovery time shown in Figure 2b is the time required for the limiter diode to change from its high attenuation state (low impedance) to its low attenuation state (high impedance). During this period the carriers in the i-region are recombining. A measure of the recovery time is the ambipolar carrier lifetime. Caverly (7) describes both the traditional technique and a new technique using the diode reactance at RF for determining the lifetime for p-i-n diodes. The technique works for diodes whose i-region thickness h is less than approximately 1.5 times the recombination length L. Caverly provides an experimental test to assure that $h/L \leq 1.5$. One advantage of this technique over the traditional technique is the parasitics of the measurement circuit do not limit the accuracy for thin i-region diodes. P-i-n diodes with 1 μm i-region thickness can have a lifetime of the order of a nanosecond.

Diode Limiter Circuits

Figure 1 shows many configurations of diode limiter circuits. Figure 1(a) has been discussed previously. Figure 1(b) is a single-diode circuit in which the rectified current flows through the inductor. Note that since the diode's impedance is lowered at high signal levels throughout the cycle, the single diode does not rectify the positive or negative peak voltages on the transmission line; if that were the case, the maximum isolation would be only 3 dB. The inductor's reactance X_L should be high at the operating frequency, but have a low inductance at frequencies associated with the build-up of the rectified current to allow the rectified current to build up rapidly, thereby reducing spike leakage.

In waveguides, the *p–i–n* diode is mounted parallel to the electric field lines in the lowest-order mode on an inductive post. The equivalent circuit in Fig. 1(c) shows the reactances of the post in shunt with the waveguide impedance Z_w. For self-activated limiter operation, the low-pass filter for inserting the dc bias is not needed. The limiters shown in Fig. 1(a–c) reflect most of the incident power back toward the source. If this reflected power is undesirable (e.g., an application in which a limiter is used for stealth purposes), a nonreflective limiter [i.e., a power-dependent attenuator, as shown in Fig. 1(d)] may be required. A nonreflective design developed by Glenn et al. (8) is self-activating but does not provide the same amount of isolation that reflective limiters provide. The nonreflective design is parallel resonated by the L and C at high signal levels, for added isolation. Nonresonant, nonreflective circuits using resistors are possible; however, resistors provide only moderate levels (10 dB to 15 dB) of isolation.

Where spike leakage is a significant problem at high-power levels, the delay line limiter [Fig. 1(e)] rectifies a sample of the large signal and applies a dc bias to the *p–i–n* diode, lowering its impedance before the intense signal arrives. The delay line may be implemented in a low-loss coaxial cable yielding an approximate 3 ns delay per meter.

Figure 1(f) shows the duplexer application for a pulsed, monostatic radar receiver protector. At normal receive-signal levels, the balanced duplexer design employs two 3 dB, 90°, hybrid couplers to split the input signal between two diode limiters. Since the limiters are in their high-impedance state, the signals are recombined at the output into the receiver input. If an intense receive signal is present, the *p–i–n* diodes conduct, and the signal is reflected back into the transmitter's circulator stage, where it is absorbed in the matched load. During transmit, the *p–i–n* diodes are low impedance and reflect the power out of the antenna port. If the antenna VSWR is high, the transmitter power is re-reflected by the diodes and is absorbed in the load of the three-port circulator. This duplexer circuit uses all passive components. If desired, the *p–i–n* diodes can be externally biased during the transmitter's pulse. If a dc path for the rectified *p–i–n* diode current is not available through the 3 dB hybrids, one must be provided via shunt inductors or other bias circuitry.

In Fig. 1, all diodes assume no package parasitics. These package parasitics [see Fig. 1(g)] can have a significant effect at microwave frequencies. The *p–i–n* diode is represented by the variables C_j and R_j, where C_j is small (typically less than 1 pF) and R_j is large at low signal levels. At high signal levels, R_j is small (typically several ohms), thereby shunting C_j. R_s represents the series contact resistance of the diode and the resistance of the inductive bond wire L_s to the diode chip. C_p is the package capacitance. Additional details of limiter design in microstrip and waveguide configurations are found in White (9) and Garver (4).

Table 2. Single-Pulse Damage Levels for *p-i-n* Diode Limiters

i-region Thickness	Pulse Length	Frequency (GHz)	Damage level (kW)	Damage Observed
0.5	10 ns	2.7	30	V_b reduced 1 V
1	1 μs	9.4	0.2	V_b reduced to 12 V
1	1 μs	3.3	1.1	V_b reduced to 25 V
2	10 ns	2.7	135	V_b reduced to 10.5 V
5	10 ns	2.7	>330	No damage up to 300 kW
10	1 μs	9.4	10	V_b reduced to 9 V

Unexpected Effects

Some limiters exhibit a hysteresis effect when operated CW, or with long pulses, as sketched in Fig. 4. The sudden increase in the isolation above an input-power threshold is retained as the input power is reduced, until the input power equals the value marked A in Fig. 4. If the power is increased again, the original input–output curve is retraced and the threshold can be observed. However, if the input power is not reduced to point A, the lower input–output curve is followed, and a threshold cannot be observed. A plausible explanation, based on space-charge effects, is given in Ward et al. (2); however, the hysteresis effect needs further experimental investigation.

When connected to high-Q circuits (e.g., filters), limiters may exhibit the nonlinear dynamic effects (chaos) of period doubling and noisy behavior. This behavior was first observed with a limiting filter that utilized a *p–i–n* diode as a capacitive reactance at the output of a microwave filter structure developed by Tan (10). Unexpected signal generation by a limiter appears to be avoidable above 1 GHz by using i-region thicknesses exceeding 3 μm and a circuit Q less than 100. Further experiments and analyses are needed to fully understand and alleviate this device–circuit interaction.

Limiter Burn-Out Levels

The CW burn-out level of a commercial *p–i–n* diode limiter is usually only a few watts. It is recommended that the CW power specification not be exceeded since the diode may be operating above its maximum junction temperature or the mounting solder could melt. The same power limitation applies to pulse lengths long compared to the thermal response time of the diode.

Most limiters are also specified for pulsed operation with 1 μs pulse length at 0.1% duty cycle (1000 pps). In general, these ratings are conservative and can usually be exceeded by 3 dB.

Table 2 shows the burn-out level results of a limited number of experiments in 50-ohm coaxial circuits for *p–i–n*

diode limiters with varied-thickness *i*-regions. Damage was observed in three stages: (1) reverse current increases causing reduced reverse breakdown voltage, (2) as the diode impedance became lower the insertion loss increased, and (3) eventually fusing occurred and the diode became an open circuit, ceasing its limiting action.

GaAs *p–i–n* diode limiters have been fabricated and their performance has been measured. There appears to be little advantage to using GaAs, since its lower thermal conductivity cannot transfer the heat generated in the diode to the heat sink as effectively as Si can. However, for GaAs monolithic microwave integrated circuits (*MMIC*) devices, where high quantities make the specialized assembly of Si technology expensive, GaAs *p–i–n* devices may be a viable alternative. Fabrication of the GaAs *i*-region is usually an additional process in manufacturing GaAs MMIC devices, incurring higher cost and possibly leading to lower MMIC yields. The reliability of GaAs *p–i–n* diode limiters have been questioned. GaAs limiters designed for high-power, high duty-cycle, pulsed operation have degraded and become lossy after a few thousand hours of operation. However, majority-carrier GaAs devices (e.g., MESFETs) do not appear to exhibit this form of degradation.

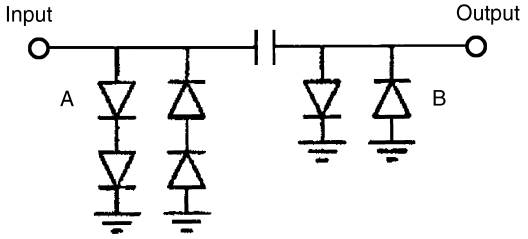

Figure 6. Two-stage Schottky limiting diode configuration (from Ref. 11).

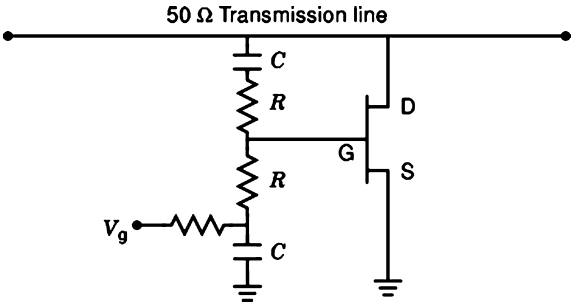

Figure 7. Schematic of a simple MESFET limiter.

Schottky Diode Limiters

MMICs are finding increasing application in today's designs when uniform performance and high quantities can justify the relatively high nonrecurring design engineering costs. Use in applications such as phased-array radars and high-volume consumer products is typical. In these applications, low-noise devices with relatively small physical dimensions are used, resulting in a susceptibility to burnout due to incident short single- or multiple-pulse energies from 0.1 μJ to 10 μJ. (Most devices can sustain a CW incident power up to 0.1 W without degradation.) A MESFET limiter that operates as a switch has been built using standard MMIC technology, to allow its fabrication along with the circuit that it must protect. This cost-effective approach avoids the requirement for employing mixed technologies (e.g., using a Si limiter with a GaAs MMIC, or adding an *i*-region fabrication step to the GaAs fabrication process).

Bahl (11) has integrated a GaAs Schottky diode limiter with a low-noise GaAs low-noise amplifier (LNA) in a MMIC format. The limiter portion of the circuit employs a two-stage Schottky limiting diode configuration as shown in Figure 6. The first stage (A) consists of large Schottky diodes in a series-anti-parallel shunt configuration capable of handling 5 W of CW incident power. The second stage (B) uses smaller anti-parallel devices in shunt with the transmission line to limit the leakage power below 0.1 W. Unlike PIN diodes, these Schottky diodes clip the peaks of both polarities of the input voltage. The added capacitance of these diodes is integrated into the input matching circuit of the LNA. The limiter performed with more than 10 W of CW incident power. The measured performance of the limiter/LNA circuit over the 8.5 to 11.5 GHz frequency range yielded a small-signal gain in excess of 14 dB, a noise figure less than 2.7 dB, and a return loss greater than 20 dB. The recovery time for a 10 W incident pulse was measured to be less than 40 ns (12).

MESFET Limiters

The GaAs MESFET limiter circuit in Fig. 7 shunts the transmission line to ground when the gate voltage allows current from drain to source. Note that the location of the drain and source change each half-cycle, based on the instantaneous polarity at the limiter's terminal connected to the transmission line. The MESFET is operated in a bidirectional mode, since no dc bias is required on the transmission line. The *R–C* voltage divider network that biases the gate is high impedance (typically, $40Z_o$ Ω). The bias port (V_g) may be used as a switch in applications for which the presence of the high-power incident pulse is known a priori (e.g., the transmitter's pulse in a phased-array radar). When V_g is grounded, a depletion-mode MESFET exhibits low impedance across the transmission line, protecting the front end when not in use. An enhancement-mode version of the MESFET limiter has been developed (13). It operates in a similar fashion to the *p–i–n* diode limiter and requires no external bias in the low-loss state.

When the gate is back-biased at small signal levels, the MESFET represents a small capacitance, consisting of the drain-to-gate and gate-to-source capacitances in series, in parallel with the drain-to-source capacitance. These capacitances are proportional to the gate width for a given MESFET technology. When the gate is not back-biased, the saturated drain-to-source current (I_{dss}) and the drain-to-source resistance are also proportional to the gate width. As a result, the designer performs a tradeoff of the amount of shunt MESFET capacitance allowed across the transmission line, to the peak current that the MESFET can pass (which, in turn, sets the power limit rating) in order to determine the gate width of the MESFET. A typical design (e.g., using a 1 mm gate width) will have an insertion loss less than 1 dB at 10 GHz and sink 0.2 A peak. The

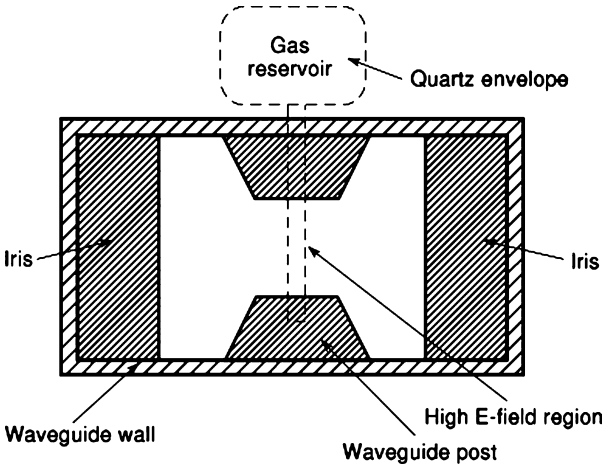

Figure 8. Cross section of a gaseous limiter in waveguide.

insertion loss decreases at lower frequencies because the MESFET's capacitive reactance shunting the transmission line increases. Larger MESFET widths allow more current with increased insertion loss.

Simple limiter circuits have been refined for specific applications by Vasile (14) and by Podell and Stoneham (15).

GASEOUS LIMITERS

Gaseous limiters are able to operate over a wide range of incident power levels from a few watts to megawatts. For this reason, gaseous limiters are the technology of choice for the highest power applications throughout the microwave spectrum. Most gaseous limiter designs have a few percent bandwidth and are suitable for radar receiver protector applications. However, a new TEM design has low insertion loss over several octaves bandwidth.

Gaseous limiters use the breakdown of a gas in a high electric field to change the impedance across a transmission line. The typical high-power waveguide design shown in Fig. 8 places a quartz tube filled with a noble gas (typically, Ar) across the waveguide gap at the point of the highest electric field. The capacitance of the posts is cancelled by the inductance of the iris in the waveguide. These two reactances limit the bandwidth to a few percent. Other designs use waveguide windows to contain the gas in the post region. The window design has a lower lifetime because of the increased absorption cross section of the gas (or gas cleanup) with the metal (typically, Ni) walls, resulting in reduced gas pressure and performance. Because the quartz-absorption cross sections are several orders of magnitude smaller than those made of metals, gaseous limiters using quartz gas reservoirs have useful lifetimes usually exceeding 20 years.

At electric field intensities below the arc threshold, the posts and iris appear to be a resonant circuit across the waveguide. The gaseous pressure, mixture, and electric field intensity in the presence of "seed" electrons set the threshold for the arc. When the arc occurs, the increased conductance across the posts presents a severe mismatch to the waveguide impedance, resulting in significant reflected power. The arc absorbs about 7% (10%, worst case) of the incident power, resulting in heat that must be conducted through the quartz tube to the walls of the waveguide posts. Because quartz has a high melting point, pulsed operation with hundreds of kilowatts incident is possible. The gas pressure and mixture is adjusted according to the Paschen curve for the desired arc threshold. The seed electrons are provided by a radioactive source or a small microwave oscillator. The tritium source (typically 100 mCu) emits electrons with a half-life of 12.6 years. Since only a few electrons are needed to initiate the arc, the tritium is useful for three half-lives. The tritium is positioned to irradiate the gas between the posts. Goldie and Patel (16) used a small microwave oscillator that continually excite enough gas molecules to provide the "seed" electrons. When Ar is used for the gas the threshold is several watts, with a recovery time of several milliseconds. If the Ar recovery time is too long, a chlorine–oxygen mixture may be used in which the electrons and ions recombine faster (typically, within 100 ns), and the arc loss is lower, but the arc threshold is higher (10 W to 20 W). If the flat leakage of the gaseous limiter is too great, *p–i–n* limiters may be cascaded to remove the spike leakage and lower the flat leakage to an acceptable level.

The wideband gaseous limiter operates on the same principle as the narrowband device. Patel et al. (17) configured a suspended, 50 Ω, stripline with the gas mixture surrounding the transmission line. Units with 6 W to 8 W thresholds and 50 W of average power have been built. The device operates over a 30% bandwidth primarily limited by coax-to-stripline transitions at the ports.

FERRITE LIMITERS

Ferrites (e.g., yttrium iron garnet or YIG) are used for tunable filters and other applications. These filters are narrowband devices in which the magnetic spin vectors (magnetic dipoles) of the ferrite are oriented by an externally applied magnetic field (typically, 100 Oe) that can be varied to change the resonant frequency of the filter. The spins on the lattice sites are also coupled to the magnetic field of a microwave signal. If the strength of the signal's magnetic field exceeds a threshold, energy from the signal's magnetic field is coupled to the spin vectors of the fixed lattice ions, thereby creating spin waves. These spin waves are able to transfer energy to heat the lattice, removing energy from the incident microwave signal. The process is nonlinear, with respect to incident microwave magnetic field strength, and yields substantially different performance as a microwave limiter. Lax and Button (18) stated that limiting thresholds vary from −25 dBm to 50 dBm. Section VI of Adam, et. al., (19) gives additional information regarding these nonlinear magnetic microwave devices. Ref. 19 is an excellent overview of ferrite technologies [see also MICROWAVE FERRITE MATERIALS].

Carter and McGowan (20) developed a limiter consisting of a ferrite slab mounted against the narrow wall of a waveguide with a 1500 Oe externally applied magnetic field. This ferrite limiter was able to dissipate 10 kW incident pulses. The insertion loss over the 8.9 GHz to 9.5

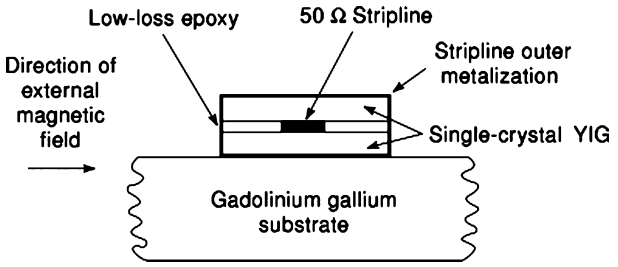

Figure 9. Cross section of a frequency-selective limiter.

GHz range was less than 1 dB. The threshold power and flat-leakage power levels were 28 W. At 10 kW incident power, the spike energy was 3 μJ with a spike power level of 2.9 kW. The recovery time was less than 20 ns, which is much shorter than that of a gaseous limiter. The threshold and flat-leakage power levels were reduced to <30 mW with the addition of a varactor (thin i-region p–i–n diode) limiter behind the ferrite limiter.

Because of their tunability by varying the externally applied magnetic field by at least an octave, ferrite filters can be used as frequency-selective limiters. They have the ability to attenuate a signal at a frequency selected by the magnitude of the external field, while providing minimal attenuation at nearby frequencies. Adam and Stitzer (21) determined that the bandwidth of the limiting frequencies (typically, 50 MHz) is related to the linewidth of the spin-wave coupling. A frequency-selective limiter will attenuate an intentional jamming signal, while an electronic warfare receiver is able to listen to signals on nearby frequencies.

A stripline configuration of the frequency-selective limiter was developed by Adam and Stitzer (21) using single-crystal YIG in place of the usual microwave dielectric material, as shown in Fig. 9. The limiting threshold was about 20 dBm. The ultimate limiting capability of this technique appears to be in the 15 dB to 20 dB range. By cascading limiter, amplifier, limiter, and so on, they demonstrated that an incident power range of 60 dB could be compressed to a dynamic range of less than 5 dB. A frequency selective limiter operating in the 400 to 800 MHz range (22) has been developed with a threshold power level for limiting 100 times lower (≈ -25 dBm) than achieved with stripline devices. The interactions between two simultaneous signals are only significant if their frequency separation is less than 10 MHz. These units are built using the magnetostatic surface wave propagation in a GaScYIG film.

OTHER LIMITER TECHNOLOGIES

The limiter technologies in this section, except for the multipactor, are very experimental in nature and have not been produced in quantity. These limiters are presented here to document their existence and to present very preliminary results.

Multipactor

Experimentation has taken place using numerous other technologies, with mixed success. A summary of some of the technologies appears in Table 3.

Table 3. Other Limiter Technologies

Technology	Performance	Status
Multipactor	Excellent, requires external biases	Implemented in waveguide configurations
Bulk Window™ switch array	Excellent millimeter wave switch	Limiter performance untested, difficulty making thin i-region
Electro-optic	Fair, requires laser and optics	Relatively high insertion loss
Superconductor	Fair, 50 ns turn-on	Demonstrated at 10 GHz
Field-emitter array limiter	Unknown	Needs fabrication on low-loss substrate
Varistor paint	Unknown	Initial attempts failed
Temperature-dependent resistor	Fair	Only analyzed to date

The multipactor takes advantage of secondary electron resonance (multipacting) to provide low impedance across a waveguide [see FIELD EMISSION]. The multipactor is usually configured as the first stage of a two-stage limiter, since it limits the power to only several watts. The second stage is a p–i–n diode limiter, with a flat leakage of less than 100 mW.

Multipacting is an electron-avalanche phenomenon operating in a vacuum. The multipacting region allows electrons in an alternating electric field to flow across a gap in less than a one-half cycle of the field. Both surfaces of the gap are coated, so that the secondary electron emission coefficient δ is greater than 1. The incident electric field accelerates the electrons toward one of the gap surfaces. As these initial electrons N_i strike the surface, the RF field changes sign, and the secondary electrons δN_i are accelerated toward the opposite surface. The speed at which the multipactor ignites is $N = N_i\delta^{2tf}$, where t is the time and f is the frequency (in hertz) of the electric field. Electron multiplication continues until a space charge in the gap inhibits additional electrons from being emitted from the gap's surfaces. At 10 GHz, the saturated electron density of 3×10^{10} electrons/cm^3 is achieved in 0.6 ns. The impinging RF field is reflected by the lower impedance in the gap region and is absorbed by conversion to heat in the electron cloud.

The multipactor gap consists of low-Q resonators in a combline filter configuration. An electron source emits enough electrons (N_i) into the gaps to cause the multiplication to begin on the first few cycles of RF. A supply of oxygen is leaked into the gap region so that the metal oxides continue to have a coefficient δ, since prolonged electron bombardment of the surface reduces the oxides to the metal with low δ. To counter this leak of oxygen, a small ion pump is required. The pump maintains a vacuum pressure suitable to enable the electrons to be accelerated across the gap without colliding with the oxygen molecules. Clearly, the multipactor is a more complex limiter than the others discussed here. Therefore, it has found only limited application where biases for the ion pump are already available. The multipactor operates within the band pass of the combline filter, while the filter protects the receiver's front end from intense signals out-of-band. Measured performance of a 9.6 GHz multipactor had a 12% bandwidth

(VSWR < 1.6:1), would attenuate a 50 kW pulse to a 50 mW flat leakage with a 2 μJ spike energy, and had a recovery time of less than 15 ns. Below threshold, the insertion loss was 1.5 dB, due to the combline filter (23).

Bulk Window™ Waveguide Switch Array

This switch array (or the monolithic diode array) was developed by M/A-COM Semiconductor Products (now part of Tyco Electronics), Burlington, MA, as a low-loss millimeter-wave switch for use in waveguide applications. The switch consists of a matrix of Si *p–i–n* diodes grown monolithically onto an insulting Si substrate. The substrate acts as a carrier, which is attached to a waveguide flange with suitable contacts to apply bias to the switch. The few attempts to operate the switch array as a self-activated limiter have not been successful, apparently because the *i*-region could not be designed thin enough at millimeter-wave frequencies to allow the microwave energy to lower the impedance of the *p–i–n* diodes. However, with external bias, the switch array has sustained operation at 1 kW pulse and 20 W levels at 94 GHz, with a low signal-level insertion loss of only 1 dB (24).

Electro-optic

The electro-optic limiter uses a coplanar waveguide transmission line configuration on an electro-optically active, semi-insulating semiconductor as the switched medium (25). When illuminated with photons that have sufficient energy to excite electron–hole pairs, the coplanar transmission line becomes lossy and absorbs most of the incident power. This limiter design is complicated because it requires an intense light source (e.g., a laser) to create enough electron–hole pairs to provide the level of conductivity modulation of the substrate. The light source is activated above a threshold established by external circuitry coupled to the coplanar line, similar to the delay-line limiter shown in Fig. 1(e). An implementation of this limiter design in semi-insulating Si yielded more than 30 dB isolation at 1.7 GHz, with over 100 mW of optical power. The isolation bandwidth was 25%. With no optical illumination, the same limiter had a high insertion loss of 6.5 dB, which was probably due to the high series resistance of the center conductor of the coplanar transmission line.

Superconductor

High-T_c superconductor (*HTSC*) films with a superconducting-to-normal transition at 86 K have been fabricated that show a surface resistivity change of 10^5. Gaidukov et al. (26) fabricated a two-element filter in a 8.0 GHz to 12.4 GHz rectangular waveguide. The filter used resonant irises spaced a quarter-wavelength apart, fabricated with HTSC film strips across the opening of each iris. In the superconducting state, the film strip appears as a resonant inductor across the iris, with an insertion loss of $\gg$1 dB. The 3 dB bandwidth is $\gg$1 GHz. In the normal state, the film strip is resistive, reducing both the Q and the resonant frequency of the iris, and yielding over 20 dB of isolation. When operated at 65 K with 0.8 μs pulses, the limiting began at 50 mW, and the pulse shape was unaffected by the limiter up to 0.5 W. With increased power levels, the pulse shape showed more attenuation later in the pulse, due to the heating of the HTSC film with a time constant ranging from 0.1 μs to 0.5 μs. The insertion loss increased about 5 dB during a pulse. If the HTSC film strips are heated with an external current, the dual iris assembly can be used as a switch.

Field-Emitter Array

Field emission from a cathode incorporating a matrix of $TaSi_2$ rods with final tip radii of curvature in the range of 1 nm to 10 nm has been measured at dc. Kirkpatrick et al. (27) showed that the parameters of the Fowler–Nordheim relation depend on the magnitude of the electric field at the tip. The emission is fast enough to be useful at microwave frequencies, when configured as a suspended 50 Ω microstrip (cathode) above a ground plane (anode). The $TaSi_2$ rods are mounted in an insulating Si substrate. For the limiter application, Glenn et al. (28) used a configuration similar to that shown in Fig. 9, with a vacuum replacing the YIG and a microstrip-to-ground plane spacing of 40 μm. When the electric field at the tips exceeded a threshold, electrons were emitted that shunted the transmission line, thereby operating as a limiter. As expected, the device worked with a dc threshold voltage of ≈200 V, providing limiting above 400 W on a 50 Ω transmission line. The device showed a high insertion loss at 1 GHz, which was attributed to losses in the Si substrate.

Two other limiter circuit technologies have been proposed, but have not been demonstrated to date: varistor paint and temperature-dependent resistor. The first technology uses the coplanar waveguide configuration with a varistor paint, shunting the center conductor to the coplanar ground planes. Initial attempts to build this device failed, because the fringing electric field from the coplanar line was too low to activate the varistor paint.

The second technology is a highly temperature-dependent resistor (e.g., tungsten) with a small thermal mass, in series with a transmission line. The limiter could be used in series with, or in place of, the bond wire of a susceptible microwave component. However, experimental results indicated that the shunt capacitance of the temperature-dependent resistor was too high, reducing the current heating in the resistor.

FUTURE ACTIVITIES

While *p–i–n* diode limiter technology is rather well-developed, several investigations still remain to be conducted. These investigations include: determining why input–output power hysteresis occurs for continuous and long-pulse operation; experiments to determine whether a slightly *p*-doped *i*-region diode will have lower spike leakage than present designs; and determining why GaAs *p–i–n* devices appear to degrade with intense pulses.

MESFET limiters must be designed to carry higher pulsed currents to enable operation above 100 W and higher CW power levels for solid-state phased array applications, without the requirement for a large gate width. Also, limiters must be developed using the low-noise

PHEMT technology, to make them compatible with the amplifiers they must protect.

Although self-activated, high-power, millimeter-wave limiters are not presently available, the monolithic diode array concept appears to be the most likely to have low insertion loss, if the thickness of the *i*-region can be reduced. Furthermore, the monolithic diode array does not increase the loss at low signal levels, due to the distribution of the carriers at the $p+$ to i and the $n+$ to i transistions.

BIBLIOGRAPHY

1. A. E. Fathy and A. Rosen, PIN Diodes, *Encyclopedia of RF and Microw. Eng.*, Vol. 4, 3858–3869, 2005.
2. A. L. Ward, R. J. Tan and R. Kaul, Spike leakage of thin Si PIN limiters, *IEEE Trans. Microw. Theory Tech.*, **42**: 1879–1885, 1994.
3. D. Leenov, The silicon PIN diode as a microwave radar protector at megawatt levels, *IEEE Trans. Electron Devices*, **ED-11**: 53–61, 1964.
4. R. V. Garver, *Microwave Diode Control Devices*, Norwood, MA: Artech House, 1978, Chap. 9.
5. N. J. Brown, Design concepts for high-power PIN diode limiting, *IEEE Trans. Microw. Theory Tech.*, **MTT-15**: 732–742, 1967.
6. R. H. Caverly and M. J. Quinn, Time Domain Modeling of PIN Control and Limiter Diodes, *IEEE MTT-S Intl. Microw. Symp. Digest*, **2**: 719–722, 1999.
7. R. H. Caverly, RF technique for determining ambipolar carrier lifetime in pin RF switching diodes, *Electronics Letters*, **34**, No. 12, 12 Nov 1998.
8. C. M. Glenn *et al.* Nonreflective limiter, US Patent No. 5, 345, 199, 1994.
9. J. F. White, *Semiconductor Control*, Norwood, MA: Artech House, 1977, Chap. 7.
10. R. J. Tan, A Limiting filter, *1991 IEEE MTT-S Intl. Microw. Symp. Digest*, **3**, 10–14 June, 1275–1278, and US Patent No. 5, 280, 256, 1994.
11. I. Bahl, 10W CW Broadband Balanced Limiter/LNA Fabricated Using MSAG MESFET Process, *Int. J. RF and Microw. CAE*, **13**: 118–127, 2003.
12. J. Looney, D. Conway and I. Bahl, An Examination of Recovery Time of an Integrated Limiter/LNA, *IEEE Microwave Magazine*, **5**: 83–86, March 2004.
13. C. Trantanella, M. Pollman and M. Shifrin, An investigation of GaAs MMIC high power limiters for circuit protection, *IEEE MTT-S Intl. Microw. Symp. Digest*, Denver, CO, June 8–13, 1997, pp. 535–538.
14. C. F. Vasile, FET adative limiter with high current FET detector, US Patent No. 5, 157, 289, 1992.
15. A. F. Podell and E. B. Stoneham, Input protection circuit, US Patent No. 5, 301, 081, 1994.
16. H. Goldie and S. Patel, An rf-primed all-halogen gas plasma microwave high-power receiver protector, *IEEE Trans. Microw. Theory Tech.*, **MTT-30**: 2177–2183, 1982.
17. S. D. Patel *et al.* Microstrip plasma limiter, *IEEE MTT-S Intl. Microw. Symp. Digest*, Long Beach, CA, June 13–15, 1989, pp. 879–882.
18. B. Lax and K. J. Button, *Microwave Ferrites and Ferrimagnetics*, New York: McGraw-Hill, 1962.
19. J. D. Adam, L. E. Davis, G. F. Dionne, E. F. Schloemann and S. N. Stitzer, Ferrite Devices and Materials, *IEEE Trans. Microw. Theory Tech.*, **MTT-50**: 721–737, 2002.
20. J. L. Carter, J. W. McGowan and X-band ferrite-varactor limiter, *IEEE Trans. Microw. Theory Tech.*, **MTT-17**: 231–232, 1969.
21. J. D. Adam and S. N. Stitzer, Frequency selective limiters for high dynamic range microwave receivers, *IEEE Trans. Microw. Theory Tech.*, **41**: 2227–2231, 1993.
22. J. D. Adam, S. N. Stitzer and R. M. Young, UHF Frequency Selective Limiters, *IEEE MTT-S Intl. Microw. Symp. Digest*, 20–25 May, 1173–1174, 2001.
23. T. P. Carlisle, X-band high-power multipactor receiver protector, *IEEE Trans. Microw. Theory Tech.*, **26**: 345–347, 1978.
24. A. L. Armstrong and Y. Anand, A limiter for high-power millimeter-wave systems, *IEEE Trans. Microw. Theory Tech.*, **31**: 238–241, 1983.
25. N. A. Riza and S. E. Saddow, Optically Controlled Photoconductive N-Bit Switched Microwave Signal Attenuator, *IEEE Micro. and Guided Wave Lett.*, **5**: 448–450, 1995.
26. M. M. Gaidukov *et al.* Microwave power limiter based on high-T_c superconductive film, *Electronics Lett.*, **26**: 1229–1231, 1990.
27. D. A. Kirkpatrick, A. Mankofsky and K. T. Tsang, Analysis of field emission from three-dimensional structures, *Appl. Phys. Lett.*, **60**: 2065–2067, 1992.
28. C. M. Glenn *et al. Microwave field emitter array limiter*, US Patent No. 6, 353, 290, 2002.

ROGER KAUL
Emeritus Corp
U.S. Army Research Laboratory
Adelphi, MD